IEEE Access
Multidisciplinary | Rapid Review | Open Access Journal

Received December 31, 2018, accepted January 9, 2019, date of publication January 21, 2019, date of current version February 6, 2019.

Digital Object Identifier 10.1109/ACCESS.2019.2893443

Fixing and Aligning Methods for Dielectric Resonator Antennas in K Band and Beyond

MA BOYUAN, J. PAN, ENHAO WANG, AND YUYUE LUO
Department of Electronic Science and Engineering, University of Electronic Science and Technology of China, Chengdu 611731, China
Corresponding author: Ma Boyuan (maboyuanmail@qq.com)

This work was supported by the Foundation for Innovative Research Group of the National Natural Science Foundation of China under Grant Nos. 61721001.

ABSTRACT Various conventional and novel fixing strategies for dielectric resonator antennas (DRAs) in K band and beyond are presented and investigated. Their effects on DRAs are studied in depth and explained theoretically through the perturbation theory and basic principles of DRAs. Multifunctional fixtures which achieve different antenna performance are then proposed and discussed. Their mechanisms for offering flexible bandwidth, miniaturization, frequency diversity, low cross polarization, and circular polarization are explained. In practical applications, glue is used besides fixtures to increase reliability, and its influence on antenna performance is difficult to predict. By considering various glue distributions in simulation beforehand, potential performance degradation is successfully mitigated. For validation, a four-element DRA array for 24-GHz automotive radars is fabricated. The results demonstrate that the proposed fixing strategy provides superior characteristics such as shock-resistance, fabrication and assembly simplicity, and robust antenna performance.

INDEX TERMS Alignment, antenna fixtures, automotive antennas, dielectric resonator antennas (DRAs).

I. INTRODUCTION

Dielectric resonator antennas (DRAs) are promising candidate in wireless systems owing to their wide bandwidth, compact size, low loss, and high degree of design freedom [1]–[3]. Moreover, since they do not suffer from ohmic or surface-wave loss, they are popular in K, Ka, millimeter-wave (MMW), THz, and optical bands [4]–[6], where communication and radar systems enjoy larger network capacity, higher data rates, and smaller size.

One typical system in both K and MMW bands is automotive radar, where short-range systems operate around 24 GHz, and mid-to-long-range ones work at 76-81 GHz [7], [8]. Due to their multiple advantages [9], [10], such as high efficiency and flexible design, DRAs are qualified for these applications. Nevertheless, jolt is common in automobiles, which requires DRAs to have adequate structural firmness [11].

Satellite communication (SatCom) in mid-to-high end of SHF band is promising in achieving high data rates everywhere for both static and moving devices [12]–[17]. To guarantee high-quality service, it requires wideband, multi-band, high-gain, or multiply polarized antennas [12]. Microstrip patch antennas (MPAs) [13], waveguide or horn antennas [14], and reflector antennas [15] are widely used in SatCom systems. Since DRAs enjoy wider bandwidth and higher efficiency than MPAs [9], [10], smaller feeding networks than waveguide antennas, and more compact size than reflectors, they are competent in SatCom. Moreover, because of their three-dimensional (3D) structure, it is easier to excite multiple resonant modes in DRAs to realize multiple polarization, wide bandwidth, multiple bands, and pattern diversity [3]–[5]. However, moving targets like terrestrial, marine, and aerial vehicles [16] often bring about drastic jolt. Satellites suffer severe turbulence during launching [17] as well. As a result, antennas without firm structure tend to break down. MPAs are etched on circuit boards with their feeding networks [13]. Waveguide antennas use flange plates and advanced machining to ensure firmness. Whereas DRAs can hardly survive in SatCom systems applied in these conditions, without reliable fixing methods.

Because DRAs are three dimensional and cannot be easily co-fabricated with printed circuit boards (PCBs), they are mostly assembled with adhesives [1]–[6]. However, conventional glue, by itself, hardly provides enough stability for practical applications [11]. Worse still, when frequency increases, the effect of fixing methods is no longer negligible. For instance, since thickness and distribution of glue are usually uncontrollable, it causes unpredictable frequency deviation [11]–[18] even if the glue is considered

during simulation. This problem can be catastrophic for narrow-band systems, and requires extra tuning techniques in practical devices.

Though multiple fixing and aligning strategies have been proposed [11], [18]–[43], their effects on DRAs in K band and beyond are not thoroughly investigated. To obtain both structural reliability and stable antenna performance, designers might spend more time choosing an appropriate fixing method rather than designing the DRA itself.

In this paper, fixing and aligning strategies for DRAs in K band and beyond are presented and investigated. Section II reviews and discusses various fixing strategies for DRAs in literatures. Novel fixing methods are proposed and their impact on DRAs are analyzed in Section III. Theoretical explanation is obtained with the perturbation theory and basic principles of DRAs. Two types of fixtures that have 1) little influence on performance or 2) extra specific functions (e.g., circular polarization and frequency diversity) are presented and discussed. Section IV focus on practical DRA applications where glue and fixtures are used together for structural firmness. Since the practical distribution of glue and its perturbation on DRAs are difficult to predict, various glue distributions are studied, based on which a mitigation method is obtained. In Section IV, a cylindrical DRA (CDRA) array for 24-GHz automotive radars is designed, fabricated and measured for validation. This study provides DRA researchers and industry with a comprehensive view of fixing and aligning strategies for DRAs in practical applications.

II. LITERATURE REVIEW

In lower microwave band, DRAs are commonly bonded to their substrates, ground plane, or feeding devices manually with nonconductive glue and soldering [18], [19]. RF conductive tapes are sometimes applied on sidewalls of DRAs to facilitate feeding and soldering [20]. Probe-fed DRAs may use the probes as fixtures. These probes are either stuck into a drilled DRA or soldered with the antenna at the sidewall [21], [22]. Although these techniques are simple and cheap, they require manual assembly. At low frequencies, these methods have acceptable error tolerance. However, when frequency increases, they often cause noticeable problems. For glue, unwanted unevenness, malposition, and air gaps change the designed resonant frequency and bandwidth of DRAs [11], [19]. Drilling and soldering require extra precision, and tapes are not suitable for tiny objects.

Several solutions are available to fix and align DRAs in K band and beyond. Lin *et al.* [23] applied raised metal borders to locate and lock radiating elements. Then, DRAs were easily adhered onto ground plane. Metal pillars were used in [24], offering extra stability and aligning accuracy. In [11], [25], and [26], drilled metal layers were used so that the DRAs were embedded in the metal ground plane. In addition, metal branches were inserted into the antenna to achieve a ''glueless'' design. However, each part of the antenna was assembled manually after separate fabrication, so that this technique is scarcely feasible beyond K band [11].

Besides metal fixtures, dielectric slabs are able to fix DRAs as well [18]. In [27] and [28], drilled dielectric slabs worked as fixing devices. Undrilled part of these slabs were either perforated densely, or had low permittivity or profile so that the DRA would not be severely perturbed. In some cases, DRAs and their dielectric fixtures are co-fabricated through 3D printing or other machining techniques. It is worth mentioning that, although 3D printing technology is widely used in fields of reflectarray and lens antennas, three dimensionally printed DRAs demand printing materials with higher permittivity to ensure good radiation [29]. Similarly, DRAs fed by coplanar mechanism can be embedded in the substrate [30], [31]. This strategy especially applies to on-chip mounted DRAs [32], [33]. To further enhance their stability and firmness, a scaffold-like 3D polylactic acid support was used to lock a spherical DRA [34]. It sacrifices simplicity for better firmness.

Substrate integrated waveguide (SIW) technology plays an important role in DRA fixing. DRAs employing this technology enjoy good accuracy, but require sophisticated design. DRAs fed by an SIW can be co-fabricated with their substrates [35]. In consequence, firmness and alignment are no longer problems. However, this technique results in large volume and limited forms. Another solution is using substrate integrated DRAs (SIDRAs) [36]–[39]. At the center of a dielectric slab, a round of air holes are drilled to mimic an isolated DRA. A set of metal vias are sometimes used at the periphery to suppress surface waves and enhance isolation [36]. Redundant part is unprocessed [37], completely removed [38], or perforated densely to lower its effective permittivity [39]–[41]. The core idea of these methods is to make the radiating structure another layer of ''substrate'' so that it is easily bonded with the substrate. Dielectric or metal screws are sometimes used at corners to enhance stability [42], [43]. By resorting multi-layer PCB technology, precision and simplicity can be further improved.

III. EXPERIMENT AND ANALYSIS OF FIXTURES

Multiple fixing methods in K band and beyond are shown in Fig.1. The original CDRA with finite ground plane seen in Fig. 1 (a) operates in its HEM11δ mode at 22.52 GHz. The electric and magnetic field (E- and H- field) of this mode is shown in Fig. 2. This CDRA has the height $h\_dr = 1.8$ mm, radius $r\_dr = 1.8$ mm, a relative permittivity of 9.9, and a 6mm∗6mm ground plane. The fixtures are made of metal, and bare or metal-clad dielectric material with the relative permittivity ε_r_fix, respectively.

A. FIXING FEET

First, metal and dielectric fixing feet shown in Fig. 1 (b) are studied. The resonant frequency of the $HEM_{11\delta}$ mode is changed. This mechanism is explained by two quasi-degenerate $HEM_{11\delta}$ modes named $E_{\parallel}$ mode and $E_{\perp}$ mode shown in Fig. 3. The two modes have electric vectors parallel and orthogonal to the fixing feet, respectively. The fixtures change the boundary condition at the fixing point. Metal feet

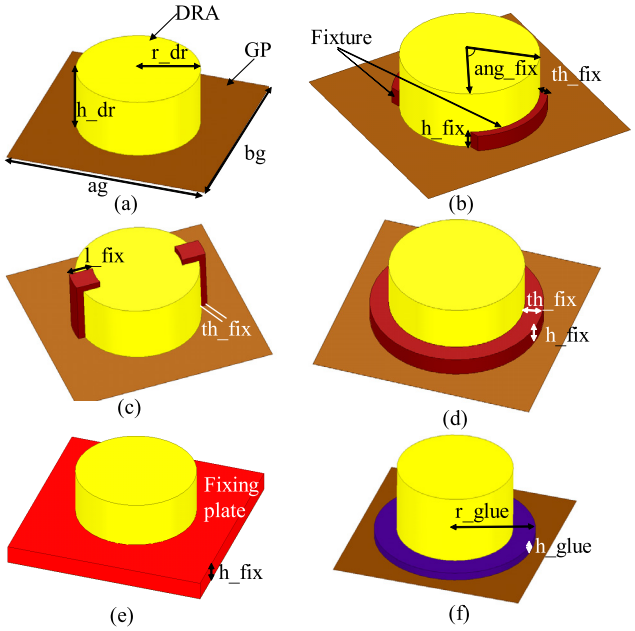

FIGURE 1. Fixing methods. (a) Original CDRA. (b) Feet. (c) Hooks. (d) Loop. (e) Plate. (f) Glue.

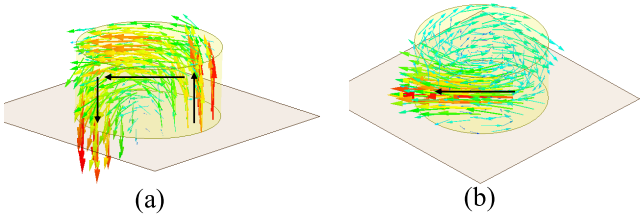

FIGURE 2. $HEM_{11\delta}$ mode of CDRA. (a) E-field. (b) H-field.

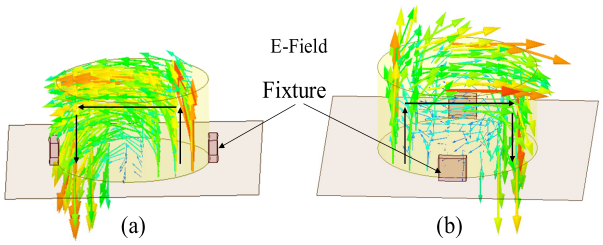

FIGURE 3. Two quasi-degenerate $HEM_{11\delta}$ modes with E-field parallel or orthogonal to fixing feet. (a) $E_{\parallel}$ Mode. (b) $E_{\perp}$ Mode.

force tangential E-field to be zero. Metal-clad and dielectric ones change the ratio of the internal and external permittivity. According to the perturbation theory [44], $E_{\parallel}$ mode is more likely to be influenced due to the concentration of E-field around the feet.

Simulation results in Fig. 4 verify this explanation. With metal feet, $E_{\parallel}$ mode is suppressed when *h_fix* is larger than 0.4 mm. Metal-clad and dielectric feet with high permittivity separate the two modes by lowering the resonant frequency of $E_{\parallel}$ mode, whereas $E_{\perp}$ mode is relatively stable in both conditions.

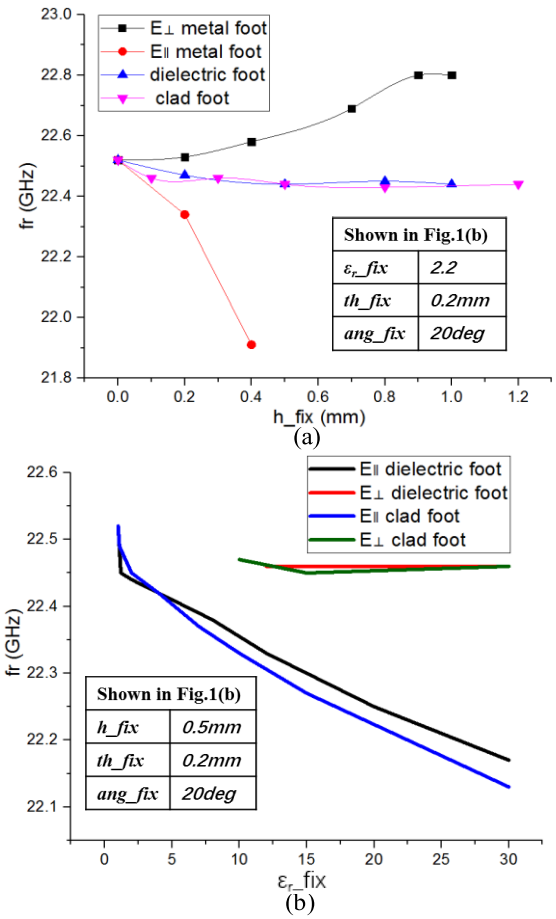

FIGURE 4. Resonant frequency of CDRA with fixing feet. (a) Feet with varying height. (b) Feet with varying permittivity.

B. FIXING HOOK

Compared to fixing feet, the hooks in Fig. 1 (c) own larger size and better stability. As shown in Fig. 5, metal hooks completely suppress $E_{\perp}$ mode. Dielectric ones are able to separate the two modes with lower permittivity. In addition, since large metal hooks contribute to confining electromagnetic field within the CDRA, they increase the resonant frequency and quality factor of $HEM_{11\delta}$ mode. In order to obtain the wanted modes, one has to be careful with the relative position between fixing feet or hooks and feeding devices. For instance, if these fixtures are expected to have little effect on a slot-fed CDRA, they should be collinear with the slot.

C. FIXING LOOP

Fixing loops can be regarded as fixing feet with an arc angle of 180 degree, as shown in Fig. 1 (d). When the bottom area of a CDRA is surrounded by a metal loop, the original $HEM_{11\delta}$ mode is significantly degraded because of the opposite boundary condition. The loop introduces the resonant mode of a circular open-end waveguide seen in Fig. 6. As a result, the original resonant frequency of $HEM_{11\delta}$ mode approaches that of the TE_{11} mode in an open-end waveguide.

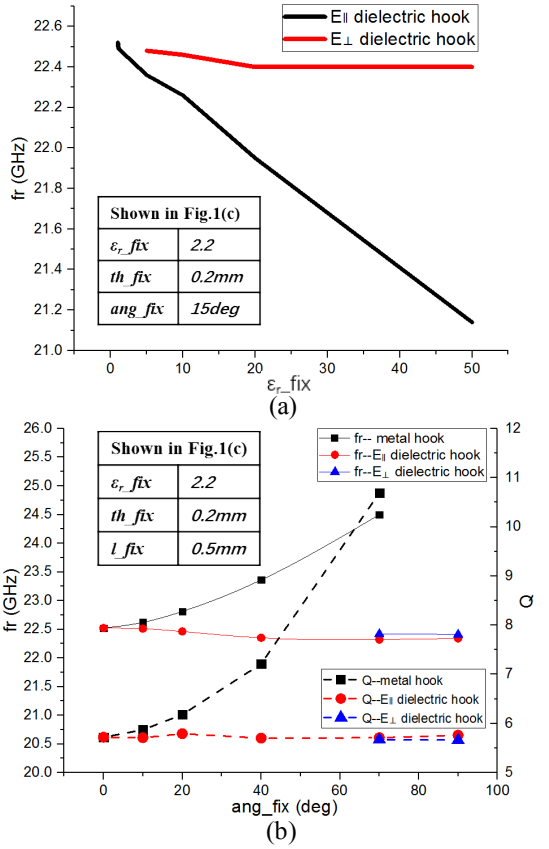

FIGURE 5. Resonant frequency and quality factor of CDRA with fixing hooks. (a) Hooks with varying permittivity. (b) Hooks with varying radian.

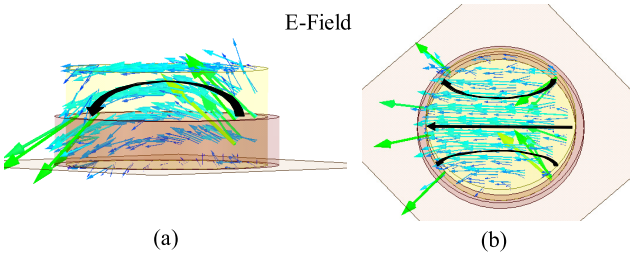

FIGURE 6. Resonant mode of CDRA with metal fixing loop. (a) Side view. (b) Top view.

As shown in Fig. 7, resonant frequency decreases as the height of the metal loop increases. Moreover, a metal loop concentrates the field within the CDRA. Consequently, the quality factor of the DRA becomes higher.

As for a dielectric loop, it helps the field leak out of the CDRA by weakening the discontinuity at the boundary, resulting in lower quality factor. If the loop is large enough, it causes surface waves. However, when a dielectric loop is coated with a metal layer, the surface wave is suppressed. Besides, a metal-clad dielectric loop introduces extra capacitance between metal layers and inductance along the metal loop. This loading effect can be utilized to optimize the performance of DRAs.

D. FIXING SLAB

Slab fixtures in Fig. 1 (e) are popular for their assembly simplicity. They are either co-fabricated with DRAs or

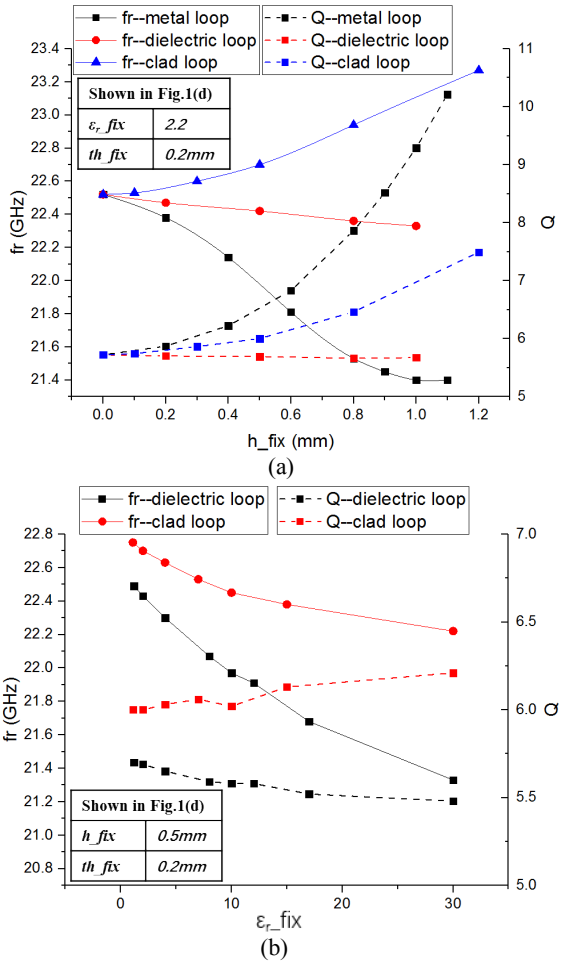

FIGURE 7. Resonant frequency and quality factor of CDRA with fixing loop. (a) Loop with varying height. (b) Loop with varying permittivity.

integrated with substrates through multi-layer PCB technology [23]–[34]. Three kinds of plates are investigated, as shown in Fig. 8. Metal slabs [11] have similar effects with metal loops. Besides introducing the resonant mode of an open-end circular waveguide presented in Fig. 6, they confine electromagnetic energy within the DRA, resulting in higher quality factor.

Dielectric slabs, in contrast, lower the quality factor since they cause surface waves bound at the dielectric-air interface. This phenomenon also enlarge the effective volume of the antenna so that the resonant frequency decreases. By coating the dielectric board with a metal layer, the surface wave vanishes. A metal-clad slab, with a hole at its center, has its own resonant modes. Therefore, the CDRA is in parallel with another resonant structure, whereas resonant characteristics of $HEM_{11\delta}$ mode vary little.

E. EFFECT-FREE AND MULTIFUNTIONAL FIXTURES

According to the above results, it is concluded that metal fixtures introduce considerable effects on DRAs. They completely change the boundary condition at the fixing point and, therefore, suppress specific or all $HEM_{11\delta}$ modes. In contrast,

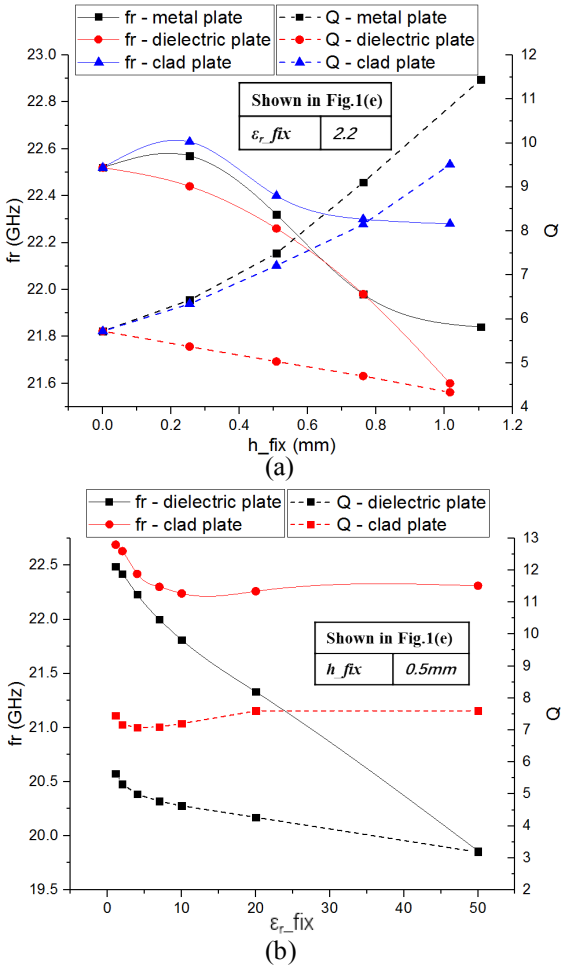

FIGURE 8. **Resonant frequency and quality factor of CDRA with fixing slab. (a) Plate with varying thickness. (b) Plate with varying permittivity.**

dielectric and metal-clad fixtures do not affect the characteristics of DRAs significantly. They slightly vary the boundary condition by changing the ratio of the internal and external permittivity. When the dielectric fixture is large enough, it introduces surface waves. By cladding it with a metal layer, these waves are suppressed.

If fixtures are supposed to have little effect on DRAs, small-size low-permittivity dielectric and metal-clad ones, e.g., fixing feet and hooks, are recommended. When fixing feet and hooks are not available, thin fixing slabs with low permittivity are preferred.

When tuning or loading effects are desired, fixtures become multifunctional devices. Diverse potential functions are concluded from the experiments. These fixtures either introduce loading effect like parasitic structures or work as extra radiating elements of hybrid or composite DRAs.

Since $E_\perp$ mode in Fig.3 is suppressed, long fixing feet and hooks reduce cross polarization by forcing CDRAs to operate in pure $E_\parallel$ mode. Through perturbation, $E_\parallel$ and $E_\perp$ modes are separated by shorter feet with a frequency interval. Therefore, better port isolation and frequency diversity performance can be obtained for multi-in-multi-out (MIMO) systems. Moreover, the perturbation introduces phase difference between these two orthogonal modes, which enables circular polarization.

Metal loops and slabs increase the quality factor of CDRAs, obtaining narrower bandwidth. In contrast, dielectric ones offer wideband performance by lowering the quality factor through enhancing wave leakage and increasing surface wave loss. Metal-clad slabs introduce extra resonant structures so that multi-band, filtering, and broadband characteristics are achievable.

As for miniaturization, Metal and thick dielectric loops or plates are capable of lowering resonant frequencies. They either introduce metal resonators, or facilitate the leakage of the internal field to enlarge the effective volume of DRAs.

Most hybrid DRAs in literatures scarcely regard the extra radiators as fixtures [1], [2]–[6], [18]. However, in order to develop DRAs enjoying both excellent performance and practicability, multifunctional fixtures are demanded.

Metal fixing feet and hooks may work as vertical monopoles and suspended dipoles, respectively. Therefore, by elaborately designing their length, wider bandwidth, multiple bands, CP waves, and flexible patterns could be attained. If MPAs or slot antennas are etched on metal-clad fixing loops and plates, composite antennas are obtained.

IV. INVESTIGATION ON GLUE

In most cases, fixtures or glue, independently, do not offer enough reliability for devices in terrestrial, aerial, or marine vehicles [11], [16], [17]. Sarkar *et al.* [11] proposed a ''glueless'' fixture, but mentioned its limitation of operating band as well. Consequently, to conquer aligning and fixing problems of DRAs near or in MMW band, fixtures and glue need to collaborate. However, because the distribution and thickness of glue are usually uncontrollable, it causes unpredicted influence on operating frequency and bandwidth of DRAs [19].

Glue and adhesives presented in Fig. 1 (f) are the most common fixing strategy to adhere DRAs onto substrates. Conductive glue and soldering are less used because they are likely to hamper feeding devices like slots and microstrip lines. Dielectric adhesives affect both feeding and antenna performance [1], [2], [19]–[21]. They fill feeding apertures, separate microstrip lines and DRAs, and change boundary conditions of the antenna. Moreover, uneven distributions of glue shown in Fig. 9 introduce air gaps at the bottom of DRAs. Instant glue and soldering particularly suffer from these phenomena. In lower bands, most of the above effects are tolerable. Nonetheless, as frequency increases, their disturbance becomes considerable. As shown in Fig. 10, when glue and adhesives are sufficient to cover the bottom side of CDRAs, conductive glue and soldering do not disturb the HEM11 δ mode since they generally maintain the boundary condition. In contrary, dielectric adhesives are more likely to change the characteristics of the antenna.

To illustrate the mechanism of dielectric glue, the effect of an air gap on DRAs needs to be explained. An air gap

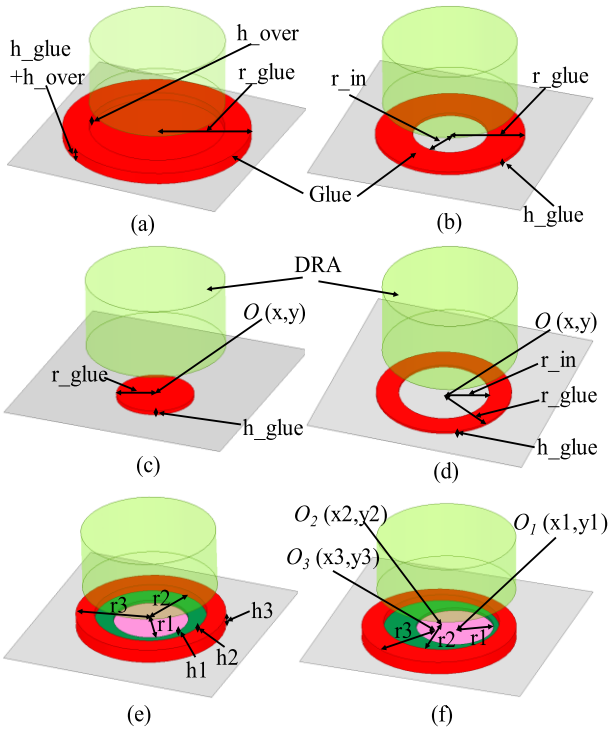

FIGURE 9. Different glue distributions in practice. (a) Overflow. (b) Ring. (c) Offset. (d) Offset ring. (e) Unevenness. (f) Offset and unevenness.

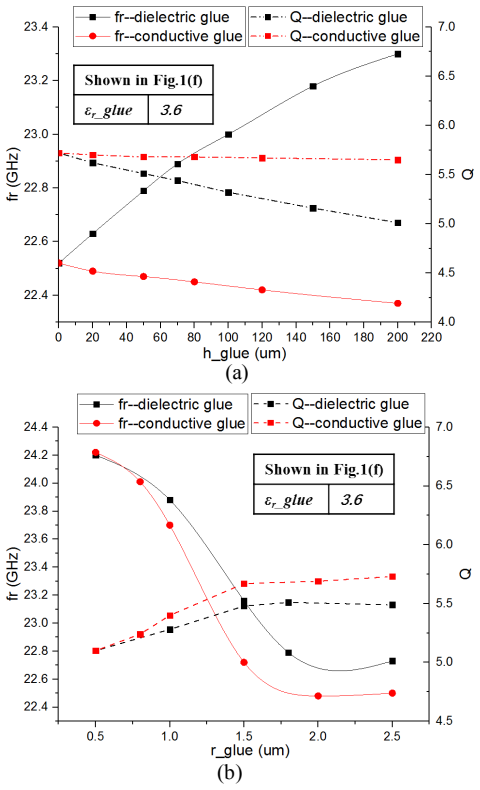

FIGURE 10. Resonant frequency and quality factor of CDRA with glues. (a) Glues with varying thickness. (b) Glues with varying radius.

between a DRA and its ground plane [1], [2] destroys the original boundary condition at the interface, i.e., a PEC that supports the $HEM_{11\delta}$ mode of a CDRA through image theory.

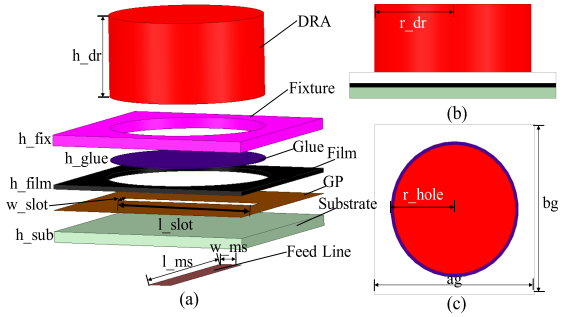

FIGURE 11. Resonant frequency and quality factor of CDRA with fixing slab.

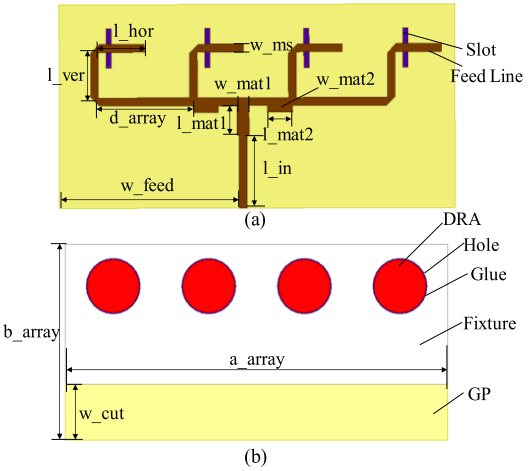

FIGURE 12. CDRA array. (a) Bottom view. (b) Top view.

This means the air gap tends to isolate the DRA and thicker air gaps lead to stronger isolation. Then, for normally incident plane waves from a denser medium (the DRA) to a thinner one (the air gap), the interface functions like a perfect magnetic conductor (PMC). Therefore, compared to CDRAs with ground plane, isolated ones in $HEM_{11\delta}$ modes have higher resonant frequencies.

Similarly, low-permittivity glue, introducing air gaps or not, increases the resonant frequency of $HEM_{11\delta}$ modes and lowers its quality factor. As the permittivity increases, the interface becomes less like a PMC. The glue is becoming an extra part of the DRA, which enlarges the equivalent volume of the antenna and lowers its effective permittivity. Consequently, the resonant frequency becomes lower. When glue and adhesives do not cover the whole bottom of DRAs, air gaps are inevitable. These gaps significantly increase resonant frequencies and decrease quality factors of $HEM_{11\delta}$ modes, as shown in Fig. 10. Nevertheless, a glue area larger than the antenna does not disturb the CDRA seriously and enjoys satisfactory error tolerance.

Various glue distributions and their simulation results are presented in Fig. 9 and Table I. It is clear that adhesives have to be considered in design and simulation. Although reproducing the simulated glue distribution during assembly is difficult, it is found that using excessive glue causes less

TABLE 1. Glue distributions and their effects.

Distributions	Parameters			f_r (GHz)	Q
None				22.52	5.72
Overflow	Conductive Glue or Soldering, h_glue=50um	r_glue (mm)	h_over (mm)		
		2	$50*10^{-3}$	22.47	5.71
		2.5	$50*10^{-3}$	22.51	5.78
		2	$150*10^{-3}$	22.43	5.81
		2.5	$150*10^{-3}$	22.5	5.93
	Dielectric Glue, ε_r =3.5, h_glue=50um r_glue=2.2mm	h_over (mm)			
		$10*10^{-3}$		22.74	5.51
		$30*10^{-3}$		22.73	5.48
		$50*10^{-3}$		22.71	5.48
		$100*10^{-3}$		22.38	5.48
		$200*10^{-3}$		22.61	5.45
Offset	ε_r=3.5, h_glue =50um	r_glue (mm)	O(x,y) (mm)		
		1	(0.3,0.8)	23.56	5.29
		1.5	(0.5,0)	23.24	5.4
		2	(0.5,0.5)	22.83	5.48
Ring	ε_r=3.5, h_glue =50um	r_in (mm)	r_glue (mm)		
		0.5	1.5	23.17	5.46
		1	1.8	22.95	5.41
		0.8	2	22.82	5.47
Unevenness	ε_r=3.5 r1, h1; r2, h2; r3, h3; (mm)	1, $20*10^{-3}$; 1.5, $50*10^{-3}$; 2, $80*10^{-3}$		23.38	5.18
		1, $80*10^{-3}$; 1.5, $50*10^{-3}$; 2, $20*10^{-3}$		23.82	5.29
Offset & Unevenness	ε_r=3.5 r1; h1, O_1 (x1,y1) r2; h2, O_2 (x2,y2) r3; h3, O_3 (x3,y3) (mm)	0.5; $80*10^{-3}$, (0.5,0) 1; $50*10^{-3}$, (0.2,0.4) 1.5; $20*10^{-3}$, (0.3,0)		24.37	5
		1; $50*10^{-3}$, (0,0.8) 1.6; $20*10^{-3}$, (0.2,0.3) 2.2; $80*10^{-3}$, (0.5,0.5)		23.53	5.16

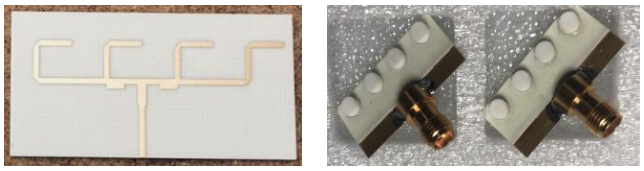

(a) (b)

FIGURE 13. Fabricated CDRA array. (a) Feed network. (b) Array.

variation than using less. Therefore, to mitigate the potential problem due to the glue distribution, unevenness and air gaps need to be avoided by applying sufficient and even excessive glue during practical fabrication and assembly.

V. DESIGN, FABRICATION AND MEASUREMENT

A four-element CDRA array with a simple dielectric fixing slab and glue is designed for 24-GHz automotive radars. The CDRA element is made of available ceramic material (ε_r = 6.8, $tan\delta$ = 0.0015) from Yangzhou Jiangjia Technology Co., Ltd, as shown in Fig. 11. The fixture and substrate are co-fabricated with Rogers RO4350B (ε_r = 3.48, $tan\delta$ = 0.0037) and bonded by a 0.1-mm Rogers RO4450B bonding film (ε_r = 3.5, $tan\delta$ = 0.004). The hole drilled on the fixture not only locates the CDRA, but also prevents glue

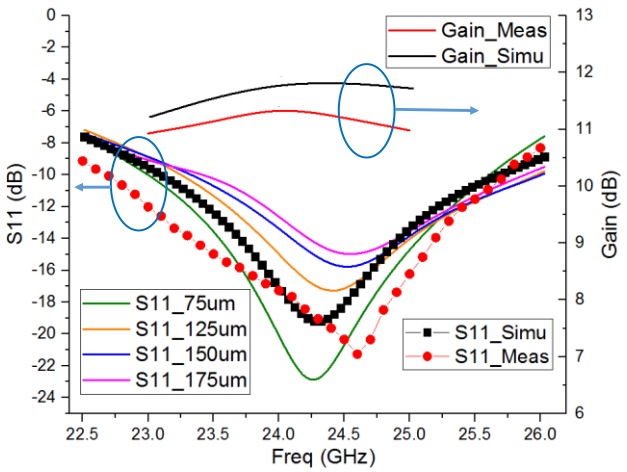

FIGURE 14. Measured and simulated gain and S_{11} parameter.

from spreading. Then, sufficient epoxy resin glue (ε_r = 3.6, $tan\delta$ = 0.004) is used to further fix the antenna.

Four elements form a linear array seen in Fig. 12. Detailed configuration is listed in Table II. The array is fed by a conventional one-to-four microstrip power divider. Part of the fixture is wiped off to facilitate feeding. The array is fabricated and manually assembled as shown in Fig. 13.

TABLE 2. Antenna configuration.

Parameter	Value	Parameter	Value	ε_r_glue	3.6	w_mat2	1.01mm
r_dr	1.9mm	h_sub	0.254mm	ε_r_dr	6.8	d_array	7mm
h_dr	1.9mm	l_ms	4.33mm	ε_r_film	3.5	l_ver	4.24mm
h_film	0.1 mm	w_ms	0.55mm	ε_r_fix	3.48	l_hor	3.27mm
h_fix	0.254mm	l_in	5mm	ε_r_sub	3.48	a_array	28mm
r_hole	2mm	l_mat1	2.04mm	ag	5 mm	b_array	14mm
l_slot	3.43mm	w_mat1	0.85mm	bg	5 mm	w_cut	4mm
w_slot	0.48mm	l_mat2	1.77mm	h_glue	0.1mm	w_feed	13mm

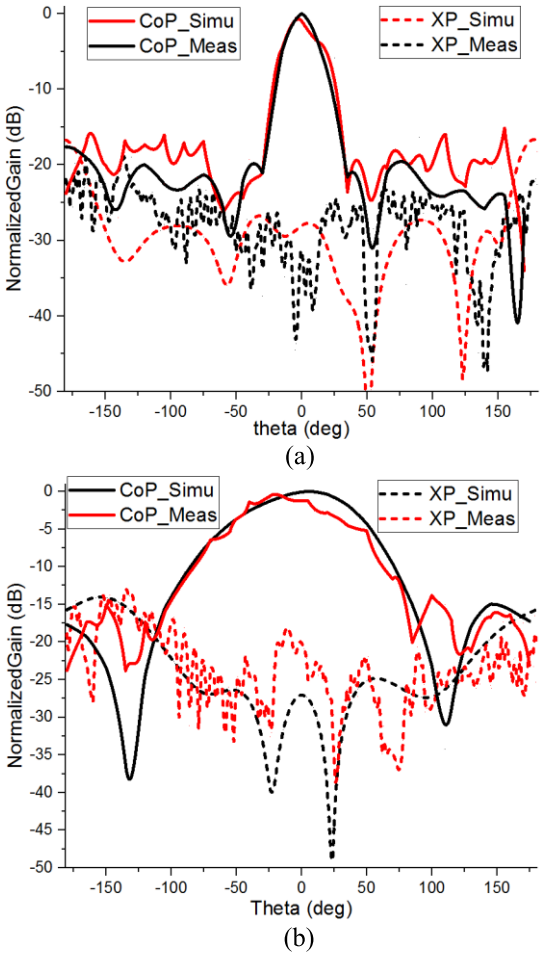

FIGURE 15. Measured and simulated radiation pattern at resonant frequency. (a) E-plane pattern. (b) H-plane pattern.

It is then measured with an Agilent vector network analyzer and a far-field measuring system in a microwave anechoic chamber of *University of Electronic Science and Technology of China*. Measurement results are presented in Fig. 14-15. With the thin fixture and sufficient glue, no obvious performance degradation is observed, implying that this fixing and aligning strategy enjoys simplicity, reliability, and high error tolerance.

VI. CONCLUSION

Multiple conventional and novel fixing methods for DRAs in K band and beyond have been presented and investigated. Plenty of research has been conducted to study the effects of various fixtures on DRAs. These effects have been summarized and theoretically explained based on the perturbation theory, and boundary condition or internal field of DRAs.

Next, effect-free fixtures and multifunctional fixtures providing flexible bandwidth, pure polarization, frequency diversity, port isolation, circular polarization, and compactness have been proposed and explained.

Then, to use glue and fixtures together for better stability, the influence of glue and adhesives have been studied with various practical distributions. It has been found that the unwanted perturbation caused by glue distribution can be mitigated.

At last, a fixing method enjoying fabrication simplicity and high error tolerance has been designed for a CDRA array applied in 24-GHz automotive radars. This work provides meaningful references for choosing DRA fixtures in K band and beyond.

REFERENCES

[1] K. M. Luk and K. W. Leung, Eds., *Dielectric Resonator Antennas*. Baldock, U.K.: Research Studies, 2003.

[2] A. Petosa, *Dielectric Resonator Antenna Handbook*. Norwood, MA, USA: Artech House, 2007.

[3] R. Kumari and R. K. Gangwar, "Circularly polarized dielectric resonator antennas: Design and developments," *Wireless Personal Commun.*, vol. 86, pp. 851–886, Jan. 2016, doi: 10.1007/s11277-015-2959-0.

[4] S. K. K. Dash, T. Khan, and A. De, "Dielectric resonator antennas: An application oriented survey," *Int. J. RF Microw. Comput.-Aided Eng.*, vol. 27, no. 3, p. e21069, 2017, doi: 10.1002/mmce.21069.

[5] S. Keyrouz and D. Caratelli1, "Dielectric resonator antennas: Basic concepts, design guidelines, and recent developments at millimeter-wave frequencies," *Int. J. Antennas Propag.*, vol. 2016, Sep. 2016, Art. no. 6075680, doi: 10.1155/2016/6075680.

[6] C. Zou, W. Withayachumnankul, M. Bhaskaran, S. Sriram, and C. Fumeaux, "Dielectric resonator nanoantennas: A review of the theoretical background, design examples, prospects, and challenges," *IEEE Antenna Propag. Mag.*, vol. 59, no. 6, pp. 30–42, Dec. 2017.

[7] W. Menzel and A. Moebius, "Antenna concepts for millimeter-wave automotive radar sensors," *Proc. IEEE*, vol. 100, no. 7, pp. 2372–2379, Jul. 2012.

[8] Y. He, K. Ma, N. Yan, Y. Wang, and H. Zhang, "A cavity-backed endfire dipole antenna array using substrate-integrated suspended line technology for 24 GHz band applications," *IEEE Trans. Antennas Propag.*, vol. 66, no. 9, pp. 4678–4686, Sep. 2018.

[9] G. Divya, K. J. Babu, and R. Madhu, "A synoptic review on dielectric resonator antennas," in *Microelectronics, Electromagnetics and Telecommunications* (Lecture Notes in Electrical Engineering), vol. 471. Singapore: Springer, 2018, doi: 10.1007/978-981-10-7329-8_19.

[10] D. Guha and C. Kumar, "Microstrip patch versus dielectric resonator antenna bearing all commonly used feeds: An experimental study to choose the right element," *IEEE Antennas Propag. Mag.*, vol. 58, no. 1, pp. 45–55, Feb. 2016.

[11] C. Sarkar, D. Guha, and C. Kumar, "Glueless compound ground technique for dielectric resonator antenna and arrays," *IEEE Antennas Wireless Propag. Lett.*, vol. 16, pp. 2440–2443, 2017.
[12] C.-X. Mao, S. Gao, Q. Luo, T. Rommel, and Q.-X. Chu, "Low-cost X/Ku/Ka-band dual-polarized array with shared aperture," *IEEE Trans. Antennas Propagat.*, vol. 65, no. 7, pp. 3520–3527, Jul. 2017.
[13] B. Lesur *et al.*, "A large antenna array for Ka-band satcom-on-the-move applications—Accurate modeling and experimental characterization," *IEEE Trans. Antennas Propag.*, vol. 66, no. 9, pp. 4586–4595, Sep. 2018.
[14] J. I. Herranz-Herruzo, A. Valero-Nogueira, M. Ferrando-Rocher, B. Bernardo, A. Vila, and R. Lenormand, "Low-cost Ka-band switchable RHCP/LHCP antenna array for mobile SATCOM terminal," *IEEE Trans. Antennas Propag.*, vol. 66, no. 5, pp. 2661–2666, May 2018.
[15] Z. Yang, K. C. Browning, and K. F. Warnick, "High-efficiency stacked shorted annular patch antenna feed for Ku-band satellite communications," *IEEE Trans. Antennas Propag.*, vol. 64, no. 6, pp. 2568–2572, Jun. 2016.
[16] J. Zhao, F. Gao, Q. Wu, S. Jin, Y. Wu, and W. Jia, "Beam tracking for UAV mounted satcom on-the-move with massive antenna array," *IEEE J. Sel. Areas Commun.*, vol. 36, no. 2, pp. 363–375, Feb. 2018.
[17] R. Baggen, S. Holzwarth, M. Bottcher, and S. Otto, "Innovative antenna front ends from L-band to Ka-band," *IEEE Antenna Propag. Mag.*, vol. 59, no. 5, pp. 116–129, Oct. 2017.
[18] C. Fumeaux *et al.*, "Terahertz and optical dielectric resonator antennas: Potential and challenges for efficient designs," in *Proc. 10th EuCAP*, Davos, Switzerland, Apr. 2016, pp. 1–4.
[19] A. M. Faiz, N. Gogosh, S. A. Khan, and M. F. Shafique, "Effects of an ordinary adhesive material on radiation characteristics of a dielectric resonator antenna," *Microw. Opt. Technol. Lett.*, vol. 56, no. 6, pp. 1502–1506, Jun. 2014, doi: 10.1002/mop.28349.
[20] S. Caizzone, G. Buchner, and W. Elmarissi, "Miniaturized dielectric resonator antenna array for GNSS applications," *Int. J. Antennas Propag.*, vol. 2016, Jun. 2016, Art. no. 2564087, doi: 10.1155/2016/2564087.
[21] Z. Chen and H. Wong, "Liquid dielectric resonator antenna with circular polarization reconfigurability," *IEEE Trans. Antennas Propag.*, vol. 66, no. 1, pp. 444–449, Jan. 2018.
[22] R. Cicchetti, A. Faraone, E. Miozzi, R. Ravanelli, and O. Testa, "A high-gain mushroom-shaped dielectric resonator antenna for wideband wireless applications," *IEEE Trans. Antennas Propag.*, vol. 64, no. 7, pp. 2848–2861, Jul. 2016.
[23] J. Lin, W. Shen, and K. Yang, "A low-sidelobe and wideband series-fed linear dielectric resonator antenna array," *IEEE Antennas Wireless Propag. Lett.*, vol. 16, pp. 513–516, 2017.
[24] Y. M. Pan, P. F. Hu, K. W. Leung, and X. Y. Zhang, "Compact single-/dual-polarized filtering dielectric resonator antennas," *IEEE Trans. Antennas Propag.*, vol. 66, no. 9, pp. 4474–4484, Sep. 2018, doi: 10.1109/TAP.2018.2845457.
[25] C. Sarkar, D. Guha, and C. Kumar, "Compound ground plane designed for probe-fed dielectric resonator antennas," in *Proc. IEEE Int. Conf. Antenna Innov. Modern Technol. Ground, Aircr. Satell. Appl. (iAIM)*, Nov. 2017, pp. 1–4.
[26] D. Guha, C. Sarkar, and C. Kumar, "Dielectric resonator antenna: A solution for its mount on metallic body," in *Proc. IEEE Int. Symp. Antennas Propag. USNC/URSI Nat. Radio Sci. Meeting*, Jul. 2017, pp. 1765–1766.
[27] A. A. Qureshi, D. M. Klymyshyn, M. Tayfeh, W. Mazhar, M. Borner, and J. Mohr, "Template-based dielectric resonator antenna arrays for millimeter-wave applications," *IEEE Trans. Antennas Propag.*, vol. 65, no. 9, pp. 4576–4584, Sep. 2017.
[28] H. Attia and A. A. Kishk, "Wideband self-sustained DRA fed by printed ridge gap waveguide at 60 GHz," in *Proc. IEEE 28th Annu. Int. Symp. Pers., Indoor, Mobile Radio Commun. (PIMRC)*, Oct. 2017, pp. 1–3.
[29] A. A. Abdulmajid, Y. Khalil, and S. Khamas, "Higher-order-mode circularly polarized two-layer rectangular dielectric resonator antenna," *IEEE Antenna Wireless Propag. Lett.*, vol. 17, no. 6, pp. 1114–1117, Jun. 2018.
[30] M. Abedian, S. K. A. Rahim, C. Fumeaux, S. Danesh, Y. C. Lo, and M. H. Jamaluddin, "Compact ultrawideband MIMO dielectric resonator antennas with WLAN band rejection," *IET Microw. Antennas Propag.*, vol. 11, no. 11, pp. 1524–1529, Sep. 2017.
[31] M. Abedian, H. Oraizi, S. K. Abdul Rahim, S. Danesh, M. R. Ramli, and M. H. Jamaluddin,, "Wideband rectangular dielectric resonator antenna for low-profile applications," *IET Microw. Antennas Propag.*, vol. 12, no. 1, pp. 115–119, Jan. 2018.
[32] Z. Ahmad and J. Hessekbarth, "On-chip mounted millimeter-wave dielectric resonator antenna," in *Proc. GeMiC*, Freiburg, Germany, Mar. 2018, pp. 142–144.
[33] D. L. Cuenca, J. Hesselbarth, and G. Alavi, "Chip-mounted dielectric resonator antenna with alignment and testing features," in *Proc. 46th Eur. Microw. Conf.*, London, U.K., Oct. 2016, pp. 723–726.
[34] B. Ahn, H.-W. Jo, J.-S. Yoo, J.-W. Yu and H. L. Lee, "Pattern reconfigurable high gain spherical dielectric resonator antenna operating on higher order mode," *IEEE Antennas Wireless Propag. Lett.*, vol. 18, no. 1, pp. 128–132, Jan. 2019, doi: 10.1109/LAWP.2018.2882871.
[35] H. Chu and Y.-X. Guo, "A novel approach for millimeter-wave dielectric resonator antenna array designs by using the substrate integrated technology," *IEEE Trans. Antennas Propag.*, vol. 65, no. 2, pp. 909–914, Feb. 2017.
[36] K. Gong, X. H. Hu, P. Hu, B. J. Deng, and Y. C. Tu, "A series-fed linear substrate-integrated dielectric resonator antenna array for millimeter-wave applications," *Int. J. Antennas Propag.*, vol. 2018, Apr. 2018, Art. no. 9672790, doi: 10.1155/2018/9672790.
[37] Y.-X. Sun and K. W. Leung, "Substrate-integrated two-port dual-frequency antenna," *IEEE Trans. Antennas Propag.*, vol. 64, no. 8, pp. 3692–3697, Aug. 2016.
[38] Y.-X. Sun and K. W. Leung, "Circularly polarized substrate-integrated cylindrical dielectric resonator antenna array for 60 GHz applications," *IEEE Antennas Wireless Propag. Lett.*, vol. 17, no. 8, pp. 1401–1405, Aug. 2018, doi: 10.1109/LAWP.2018.2847295.
[39] Y. Li and K.-M. Luk, "A 60-GHz dense dielectric patch antenna array," *IEEE Trans. Antennas Propag.*, vol. 62, no. 2, pp. 960–963, Feb. 2014.
[40] R. Movahedinia, M. R. Chaharmir, A. R. Sebak, M. R. Nikkhah, and A. A. Kishk, "Realization of large dielectric resonator antenna ESPAR," *IEEE Trans. Antennas Propag.*, vol. 65, no. 7, pp. 3744–3749, Jul. 2017.
[41] Y. Li and K.-M. Luk, "Wideband perforated dense dielectric patch antenna array for millimeter-wave applications," *IEEE Trans. Antennas Propag.*, vol. 65, no. 8, pp. 3780–3786, Aug. 2015.
[42] M. Asaadi and A. Sebak, "Gain and bandwidth enhancement of 2×2 square dense dielectric patch antenna array using a holey superstrate," *IEEE Antenna Wireless Propag. Lett.*, vol. 16, pp. 1808–1811, 2017.
[43] M. Asaadi, I. Afifi, and A.-R. Sebak, "High gain and wideband high dense dielectric patch antenna using FSS superstrate for millimeter-wave applications," *IEEE Access*, vol. 6, pp. 38243–38250, 2018, doi: 10.1109/ACCESS.2018.2854225.
[44] M. Pozar, *Microwave Engineering*, 3rd ed. Hoboken, NJ, USA: Wiley, 2005.

Authors' photographs and biographies not available at the time of publication.